Chapter

Permanent-Magnet Synchronous Machine Drives

Adhavan Balashanmugham and Mockaisamy Maheswaran

Abstract

The permanent-magnet synchronous machine (PMSM) drive is one of best choices for a full range of motion control applications. For example, the PMSM is widely used in robotics, machine tools, actuators, and it is being considered in high-power applications such as industrial drives and vehicular propulsion. It is also used for residential/commercial applications. The PMSM is known for having low torque ripple, superior dynamic performance, high efficiency and high power density. Section 1 deals with the introduction of PMSM and how it is evolved from synchronous motors. Section 2 briefly discusses about the types of PMSM. Section 3 tells about the assumptions in PMSM for modeling of PMSM and it derives the equivalent circuit of PMSM. In Section 4, permanent magnet synchronous motor drive system is briefly discussed with explanation of each blocks in the systems. Section 5 reveals about the control techniques of PMSM like scalar control, vector control and simulation of PMSM driven by field-oriented control using fuzzy logic control with space vector modulation for minimizing torque ripples. PMSM control with and without rotor position sensors along with different control techniques for controlling various parameters of PMSM for different applications is presented in Section 6.

Keywords: types of PMSM, modelling of PMSM, construction of PMSM drive systems, control techniques of PMSM, advanced topics in PMSM drives sensored control and sensorless control

1. Introduction

The electric motors are electromechanical machines, which are used for the conversion of electrical energy into mechanical energy. The foremost categories of AC motors are asynchronous and synchronous motors. The asynchronous motors are called singly excited machines, that is, the stator windings are connected to AC supply whereas the rotor has no connection from the stator or to any other source of supply. The power is transferred from the stator to the rotor only by mutual induction, owing to which the asynchronous motors are called as induction machines.

The synchronous motors require AC supply for the stator windings and DC supply for the rotor windings. The motor speed is determined by the AC supply frequency and the number of poles of the synchronous motor, the rotor rotates at the speed of the stator revolving field at synchronous speed, which is constant. The variations in mechanical load within the machine's rating will not affect the motor's synchronous speed [1].

One of the types of synchronous motor is the PMSM. The PMSM consists of conventional three phase windings in the stator and permanent magnets in the rotor. The purpose of the field windings in the conventional synchronous machine is done by permanent magnets in PMSM. The conventional synchronous machine requires AC and DC supply, whereas the PMSM requires only AC supply for its operation. One of the greatest advantages of PMSM over its counterpart is the removal of dc supply for field excitation as discussed in [2].

The development of PMSM has happened due to the invention of novel magnetic materials and rare earth materials. PMSM give numerous advantages in scheming recent motion management systems. Energy efficient PMSM are designed due to the availability of permanent magnet materials of high magnetic flux density.

In synchronous motors the rotor rotates at the speed of stator revolving field. The speed of the revolving stator field is called as synchronous speed. The synchronous speed (ω_s) can be found by the frequency of the stator input supply (f_s), and the number of stator pole pairs (p). The stator of a three phase synchronous motor consists of distributed sine three phase winding, whereas the rotor consists of the same number of p-pole pairs as stator, excited by permanent magnets or a separate DC supply source as given in [3].

When the synchronous machine is excited with a three phase AC supply, a magnetic field rotates at synchronous speed develops in the stator. The synchronous speed of this rotating magnetic field is shown by the Eq. (1).

$$\mathrm{N} = \left(120 f_s\right)/\mathrm{P}\ \mathrm{rpm} \tag{1}$$

where N, synchronous speed, f_s, frequency of AC supply in Hz; P, number of poles; p, pole pairs and it is given by ($P/2$).

2. Types of PMSM

The PMSM are classified based on the direction of field flux are as follows,

1. Radial field

2. Axial field

In radial field, the flux direction is along the radius of the machine. The radial field permanent magnet motors are the most commonly used. In axial field, the flux direction is parallel to the rotor shaft. The axial field permanent magnet motors are presently used in a variety of numerous applications because of their higher power density and quick acceleration.

The permanent magnets can be placed in many different ways on the rotor of PMSM as discussed in [3, 4]. **Figures 1** and **2** show the permanent magnets mounted on the surface of the outer periphery of rotor laminations. This type of arrangement provides the highest air gap flux density, but it has the drawback of lower structural integrity and mechanical robustness. Machines with this arrangement of magnets are known as Surface mount PMSMs.

One other types of placing the permanent magnets in the rotor, is embedding the permanent magnets inside the rotor laminations. This type of machine construction is generally referred to as Interior PMSM and it is shown in **Figures 3** and **4**.

The development of this arrangement is more difficult than the surface mount or inset magnet permanent magnet rotors. The inset permanent magnet rotor construction has the advantages of both the surface and interior permanent magnet

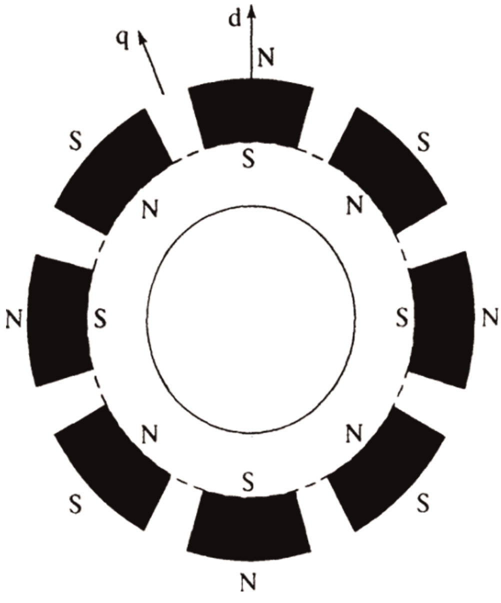

Figure 1.
Surface permanent magnet.

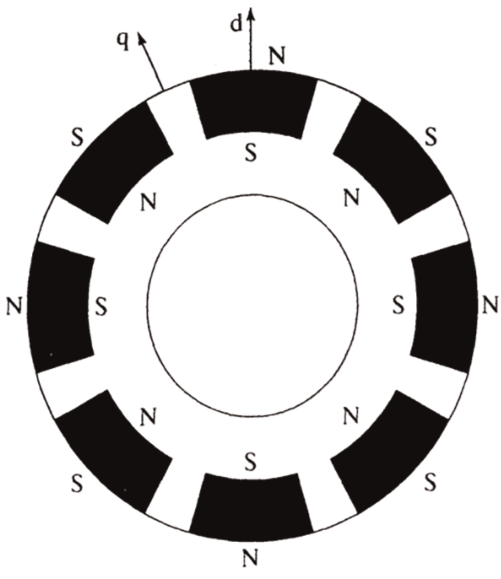

Figure 2.
Surface inset permanent magnet.

rotor arrangements by easier construction and mechanical robustness, with a high ratio between the quadrature and direct-axis inductances, respectively.

The surface PMSM with radial flux are generally applied for applications which require low speed operations. These machines have the advantage of high power density than the other types of PMSM. The interior PMSM are used for applications which require high speed.

The principle of operation is identical for all the types of PMSM, in spite of the types of mounting the permanent magnets in the rotor.

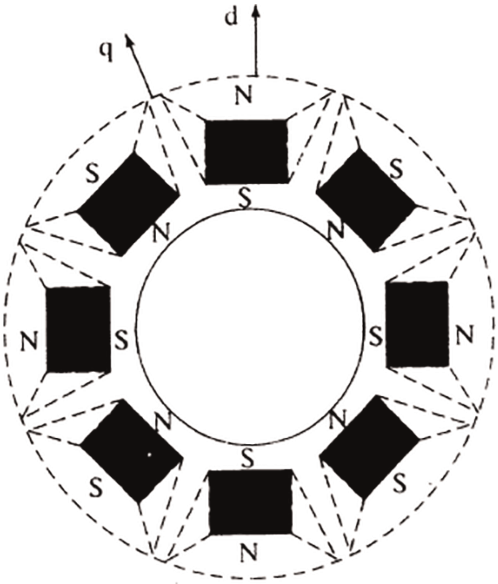

Figure 3.
Interior permanent magnet.

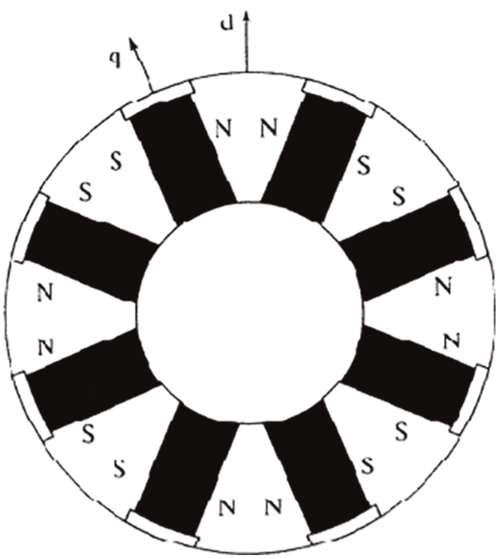

Figure 4.
Interior permanent magnet with circumferential orientation.

The important significance of the type of mounting the permanent magnets on the rotor is the variation in direct axes and quadrature axes inductance values, which is explained below. The primary path of the flux through the permanent magnets rotor is the direct axis. The stator inductance when measured in the position of permanent magnets aligned with stator winding is called as direct axis inductance. The quadrature axis inductance is measured by rotating the magnets from the already aligned position (direct axis) by 90°, in this position the iron (inter polar area of the rotor) sees the stator flux. The flux density of the permanent magnet materials is presently high and its permeability is almost equal to that of the

DOI: http://dx.doi.org/10.5772/intechopen.88597

air, such that the air gap between the rotor and stator of PMSM can be treated as an extension of permanent magnet thickness. The reluctance of direct axis is always greater than the quadrature axis reluctance, since the effectual air gap of the direct axis is several times that of the real air gap looked by the quadrature axis.

The significance of such an uneven reluctance is that the direct axis inductance is greater than the quadrature axis inductance and it is shown in Eq. (2).

$$L_d > L_q \tag{2}$$

where L_d is the inductance along the direct to the magnet axis and L_q is the inductance along the axis in quadrature to the magnet axis.

3. Modeling of PMSM

For proper simulation and analysis of the system, a complete modelling of the drive model is essential. The motor axis has been developed using d-q rotor reference frame theory as shown in **Figure 5**, as given [5]. At any particular time t, the rotor reference axis makes an angle θ_r with the fixed stator axis and the rotating stator mmf creates an angle α with the rotor d axis. It is viewed that at any time t, the stator mmf rotates at the same speed as that of the rotor axis.

The required assumptions are obtained for the modelling of the PMSM without damper windings.

1. Saturation is neglected.
2. Induced EMF is sinusoidal in nature.
3. Hysteresis losses and Eddy current losses are negligible.
4. No field current dynamics.

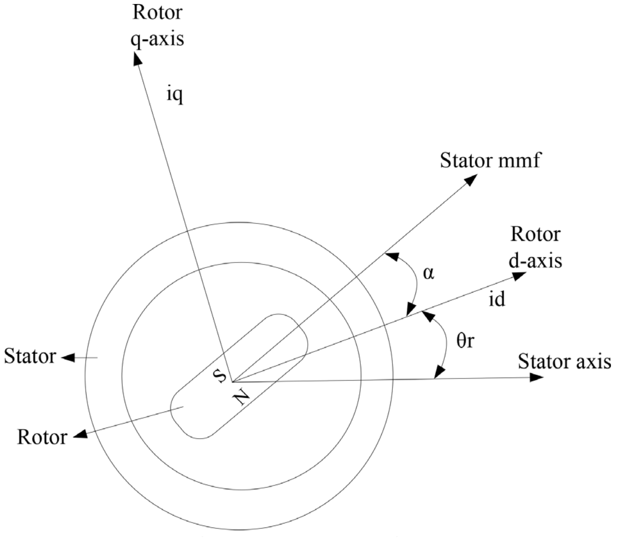

Figure 5.
Motor axis.

Voltage equations from the model are given by,

$$V_q = R_s i_q + \omega_r \lambda_d + \rho \lambda_q \tag{3}$$

$$V_d = R_s i_d - \omega_r \lambda_q + \rho \lambda_d \tag{4}$$

Flux linkages are given by,

$$\lambda_q = L_q i_q \tag{5}$$

$$\lambda_q = L_q i_q + \lambda_f \tag{6}$$

Substituting Eq. (5) and Eq. (6) into Eq. (3) and Eq. (4)

$$V_q = R_s i_q + \omega_r (L_d i_d + \lambda_f) + \rho L_d i_d \tag{7}$$

$$V_d = R_s i_d - \omega_r L_q i_q + \rho (L_d i_d + \lambda_f) \tag{8}$$

Arranging Eq. (7) and Eq. (8) in matrix form,

$$\begin{pmatrix} V_q \\ V_d \end{pmatrix} = \begin{pmatrix} R_s + \rho L_q & \omega_r L_d \\ -\omega_r L_q & R_s + \rho L_d \end{pmatrix} \begin{pmatrix} i_q \\ i_d \end{pmatrix} + \begin{pmatrix} \omega_r \lambda_f \\ \rho \lambda_f \end{pmatrix} \tag{9}$$

The developed torque motor is being given by,

$$T_e = \frac{3}{2}\left(\frac{P}{2}\right)(\lambda_d i_q - \lambda_q i_d) \tag{10}$$

The mechanical torque equation is,

$$T_e = T_L + B\omega_m + J\frac{d\omega_m}{dt} \tag{11}$$

Solving for the rotor mechanical speed form Eq. (11)

$$\omega_m = \int \left(\frac{T_e - T_L - B\omega_m}{J}\right) dt \tag{12}$$

and

$$\omega_m = \omega_r \left(\frac{2}{P}\right) \tag{13}$$

In the above equations ω_r is the rotor electrical speed, ω_m is the rotor mechanical speed.

3.1 Parks transformation and dynamic d-q modeling

The dynamic d-q modelling of the system is used for the study of motor during transient state and as well as in the steady state conditions. It is achieved by converting the three phase voltages and currents to dqo axis variables by using the Parks transformation [4].

Converting the phase voltages variables V_{abc} to V_{dqo} variables in rotor reference frame axis are illustrated in the equations,

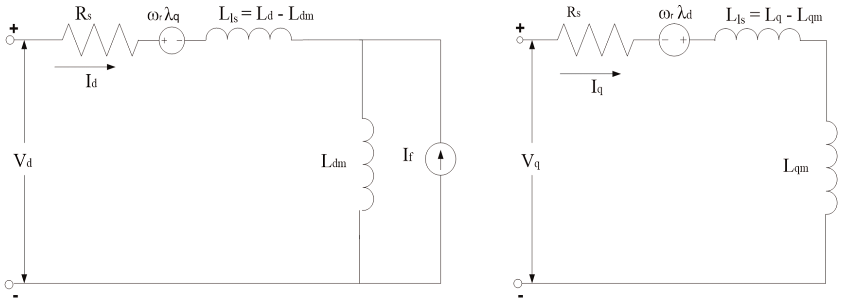

Figure 6.
Equivalent circuit of PMSM without damper windings.

$$\begin{bmatrix} V_q \\ V_d \\ V_o \end{bmatrix} = \frac{2}{3} \begin{bmatrix} \cos\theta_r & \cos(\theta_r - 120) & \cos(\theta_r + 120) \\ \sin\theta_r & \sin(\theta_r - 120) & \sin(\theta_r + 120) \\ 1/2 & 1/2 & 1/2 \end{bmatrix} \begin{bmatrix} V_a \\ V_b \\ V_c \end{bmatrix} \tag{14}$$

Convert V_{dqo} to V_{abc}

$$\begin{bmatrix} V_a \\ V_b \\ V_c \end{bmatrix} = \frac{2}{3} \begin{bmatrix} \cos\theta_r & \sin\theta_r & 1 \\ \cos(\theta_r - 120) & \sin(\theta_r - 120) & 1 \\ \cos(\theta_r + 120) & \sin(\theta_r + 120) & 1 \end{bmatrix} \begin{bmatrix} V_q \\ V_d \\ V_o \end{bmatrix} \tag{15}$$

3.2 Equivalent circuit of PMSM

Equivalent circuit is essential for the proper simulation and designing of the motor. It is achieved and derived from the d-q modelling of the motor using the voltage equations of the stator. From the assumption, rotor d axis flux is represented by a constant current source which is described through the following equation,

$$\lambda_f = L_{dm}\, i_f \tag{16}$$

where λ_f, field flux linkage; L_{dm}, d-axis magnetizing inductance; i_f, equivalent permanent magnet field current.

Figure 6 shows the equivalent circuit of PMSM without damper windings.

4. Permanent magnet synchronous motor drive system

The motor drive essentially consists of four main components such as the PMSM, the inverter, the main control unit and the position sensor. Interconnections of the components are shown in **Figure 7**.

4.1 Inverter

For variable frequency and magnitude, voltage source inverters are devices which convert the constant DC voltage level to variable AC voltage. As specified in the function, these inverters are commonly used in adjustable speed drives.

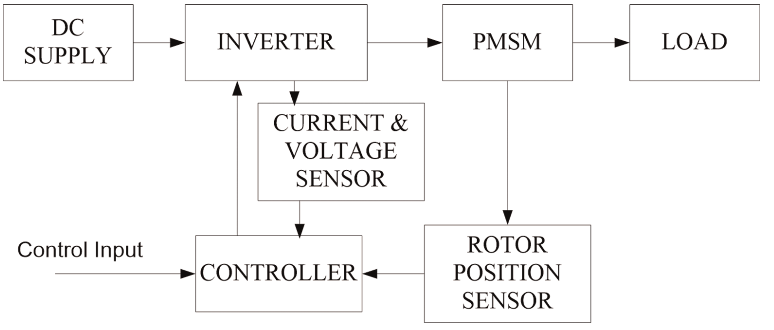

Figure 7.
Components permanent magnet synchronous motor drive.

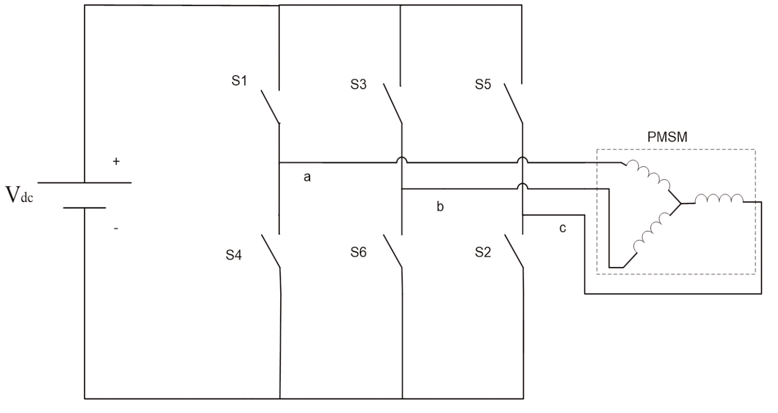

Figure 8.
Voltage source inverter with DC supply and load (PMSM).

Figure 8 shows a voltage source inverter with a supply voltage V_{dc} and with six switches. The frequency of the AC voltage can be variable or constant based on the applications [2, 6].

Three phase inverters consist of a DC voltage source and six power ON/OFF switches connected to the PMSM as shown in **Figure 8**. Selection of the inverter switches must be carefully done based on the necessities of operation, ratings and the application. There are several devices available in the market and these are thyristors, bipolar junction transistors (BJTs), MOS field effect transistors (MOSFETs), insulated gate bipolar transistors (IGBTs) and gate turn off thyristors (GTOs). It has been inferred that MOSFETs and IGBTs are preferred in the industry because of its advantages that the MOS gating permits high power gain and control advantages. MOSFET is considered to be universal power ON/OFF device for low power and low voltage applications, whereas IGBT has wide acceptance in the motor drive applications and other application in the low and medium power range. The power devices when used in motor drives applications require an inductive motor current path provided by antiparallel diodes when the switch is turned off.

5. Control techniques of PMSM

Many techniques based on both motor designs and control techniques that have been proposed in literature to diminish the torque ripples in the PMSM (**Figure 9**).

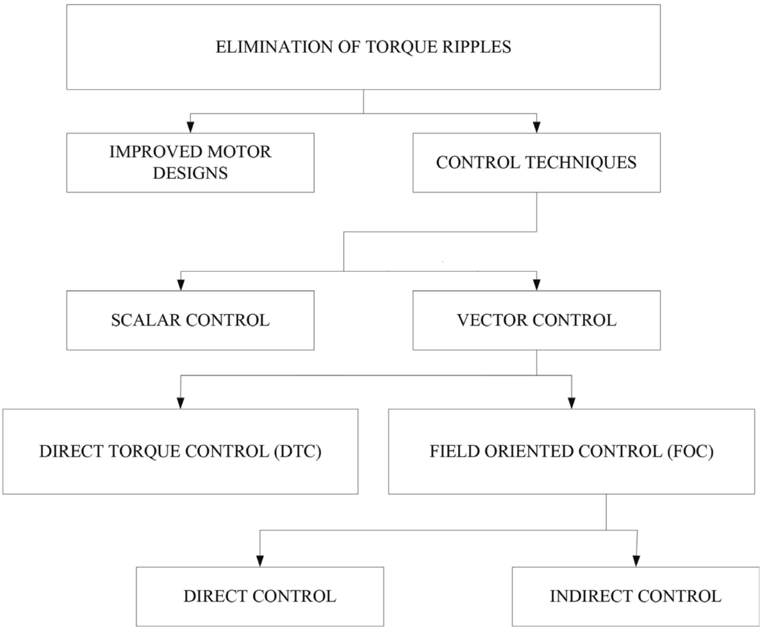

Figure 9.
Classification of the various control techniques.

5.1 Scalar control

One way of controlling AC motors for variable speed applications is through the open loop scalar control, which represents the most popular control strategy of squirrel cage AC motors. It is presently used in applications where information about the angular speed need not be known. It is suitable for a wide range of drives as it ensures robustness at the cost of reduced dynamic performance. Typical applications are pump and fan drives and low-cost drives. The main idea of this method is the variation of the supply voltage frequency inattentively from the shaft response (position, angular speed). The magnitude of the supply voltage is changed according to the frequency in a constant ratio. The motor is then in the condition where the magnetic flux represents the nominal value and the motor is neither over excited nor under excited. The major advantage of this simple method is running in a sensorless mode because the control algorithm does not need information about the angular speed or actual rotor position. On the contrary, the significant disadvantages are the speed dependence on the external load torque, mainly for PMSM, and the reduced dynamic performances.

5.2 Vector control

The vector control of PMSM allows separate closed loop control of both the flux and torque, thereby achieving a similar control structure to that of a separately excited DC machine, as discussed in [7].

5.2.1 Direct torque control (DTC)

The DTC is one of the high performance control strategies for the control of AC machine. In a DTC drive applications, flux linkage and electromagnetic torque are controlled directly and independently by the selection of optimum inverter switching modes of operation. To acquire a faster torque output, low inverter switching frequency and low harmonic losses in the model, the selection is made to restrict the flux linkages and electromagnetic torque errors within the respective flux and torque hysteresis bands. The required optimal switching vectors can be selected by using the optimum switching voltage vector look-up table. This can be obtained by simple physical considerations involving the position of the stator-flux linkage space vector, the available switching vectors, and the required torque flux linkage.

5.2.2 Field oriented control (FOC) of PMSM

For the control of PM motors, FOC technique is used for synchronous motor to evaluate as a DC motor. The stator windings of the motor are fed by an inverter that generates a variable frequency variable voltage scheme. Instead of controlling the inverter frequency independently, the frequency and phase of the output wave are controlled using a position sensor.

FOC was invented in the beginning of 1970s and it demonstrates that an induction motor or synchronous motor could be controlled like a separately excited DC motor by the orientation of the stator mmf or current vector in relation to the rotor flux to achieve a desired objective. For the motor to behave like a DC motor, the control needs knowledge of the position of the instantaneous rotor flux or rotor position of permanent magnet motor. This needs a resolver or an absolute optical encoder. Knowing the position, the three phase currents can be calculated. Its calculation using the current matrix depends on the control desired. Some control options are constant torque and flux weakening. These options are based in the physical limitation of the motor and the inverter. The limit is established by the rated speed of the motor, at which speed the constant torque operation finishes and the flux weakening starts as shown in **Figure 10** as shown in [7]. From the literature it has been found that the best control for PMSM to make it to behave like a DC motor using decoupling control is known as vector control or field oriented control. The torque components of flux and currents in the motor are separated by the vector control through its stator excitation.

From the dynamic model of the PMSM, the vector control is derived.

Assuming the line currents as input signals,

$$i_a = I_m \sin(\omega_r t + \alpha) \tag{17}$$

$$i_b = I_m \sin\left(\omega_r t + \alpha - \frac{2\pi}{3}\right) \tag{18}$$

$$i_c = I_m \sin\left(\omega_r t + \alpha + \frac{2\pi}{3}\right) \tag{19}$$

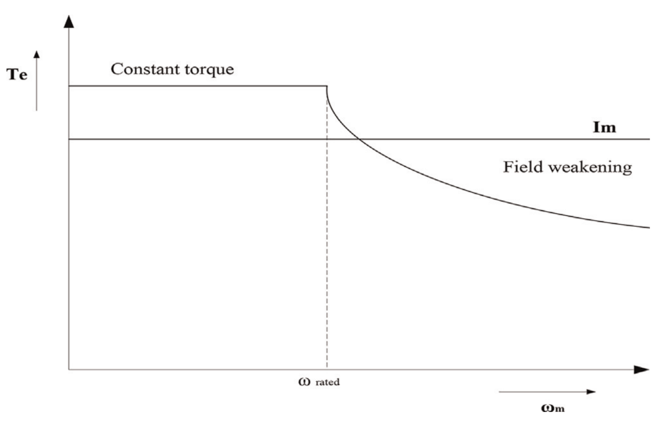

Figure 10.
Steady state torque versus speed.

Writing the above Eq. (17) to Eq. (19) in the matrix form,

$$\begin{pmatrix} i_a \\ i_b \\ i_c \end{pmatrix} = \begin{pmatrix} \cos(\omega_r t + \alpha) \\ \cos\left(\omega_r t + \alpha - \frac{2\pi}{3}\right) \\ \cos\left(\omega_r t + \alpha + \frac{2\pi}{3}\right) \end{pmatrix} (Im) \tag{20}$$

where α is the angle between the rotor field and stator current phasor, ω_r is the electrical rotor speed.

Using the Park's transformation, the currents obtained in the previous cycle are transformed to the rotor reference frame axis with the rotor speed ω_r. Since α is fixed for a given load torque, the q and d axis currents are fixed in the rotor reference frames. These constant values are made similar to the armature and field currents in the separately excited DC machine. The q axis current is distinctly equivalent to the armature current of the DC machine. The d axis current is field current, but not in its entirety. It is only a partial field current; the other part is contributed by the equivalent current source representing the permanent magnet field. Thus, the q axis current is known as the torque producing component and the d axis current is called the flux producing component of the stator currents.

Substituting Eq. (20) in Eq. (14) and obtaining i_d and i_q in terms of I_m as follows,

$$\begin{pmatrix} i_q \\ i_d \end{pmatrix} = I_m \begin{pmatrix} \sin\alpha \\ \cos\alpha \end{pmatrix} \tag{21}$$

Using Eq. (3), Eq. (4), Eq. (10) and Eq. (21) the electromagnetic torque equation is obtained as given below,

$$T_e = \frac{3}{2} \cdot \frac{P}{2} \left[\frac{1}{2} (L_d - L_q) I_m^2 \sin 2\alpha + \lambda_f I_m \sin\alpha \right] \tag{22}$$

where L_d and L_q are the d and q axis synchronous inductances. Each of the two terms in the equation has a useful physical interpretation. The first "magnet" torque term is independent of i_d but is directly proportional to the stator current component i_q. In contrast, the second reluctance torque term is proportional to the i_d and i_q current component product and to the difference of the inductance values.

As Eq. (22) shows that the torque depends on the rotor type and its inductances L_d, L_q and on permanent magnets mounted on the rotor. The non-salient PMSM have surface mounted magnets on the rotor and the reluctance term disappears since L_q equals L_d. On the contrary, the electromagnetic torque is more dominated by the reluctance component when permanent magnets are interior mounted and the rotor's saliency causes a difference in L_q and L_d.

5.2.3 Simulation of permanent magnet synchronous motor driven by field oriented control using fuzzy logic control with space vector modulation for minimizing torque ripples

One of the major disadvantages of the PMSM drive is the torque ripple produced which can be attributed to the following sources:

1. mutual torque, due to the interaction of the rotor field and stator currents;

2. reluctance torque, due to rotor saliency;

3. cogging torque, due to the existence of stator slots.

In this section presents an application of fuzzy logic control to denigrate the torque ripple associated with the field oriented control when used in control of a PMSM. a SVPWM based FOC with fuzzy logic control is proposed to produce an effective selection of the stator voltage vector to obtain smooth torque performance. The significant advantages of space vector modulation are the ease of microprocessor implementation. Also, one advantage of FOC is that it increases efficiency, letting smaller motors replace larger ones without sacrificing torque and speed. Another advantage is that it offers higher, more dynamic performance in the case of speed and torque controlled ac drives.

The block diagram of proposed FOC with the fuzzy logic based controller for the PMSM drive is shown in **Figure 11**.

The fuzzy logic controller (FLC) executes the rule based taking the inputs and gives the output by defuzzification. The inputs are torque error (e) and change in torque error (ce) and the output is torque limit (T*) which is equivalent to i_{sqref}. The dq projections of the stator currents are then compared to their reference values i_{sqref} and i_{sdref} = 0 (to get maximum torque, set to zero if there is no field weakening) and corrected by means of PI current controllers. The outputs of the current controller are passed through the inverse Park transform and a new stator voltage vector is impressed to the motor using the SVPWM technique.

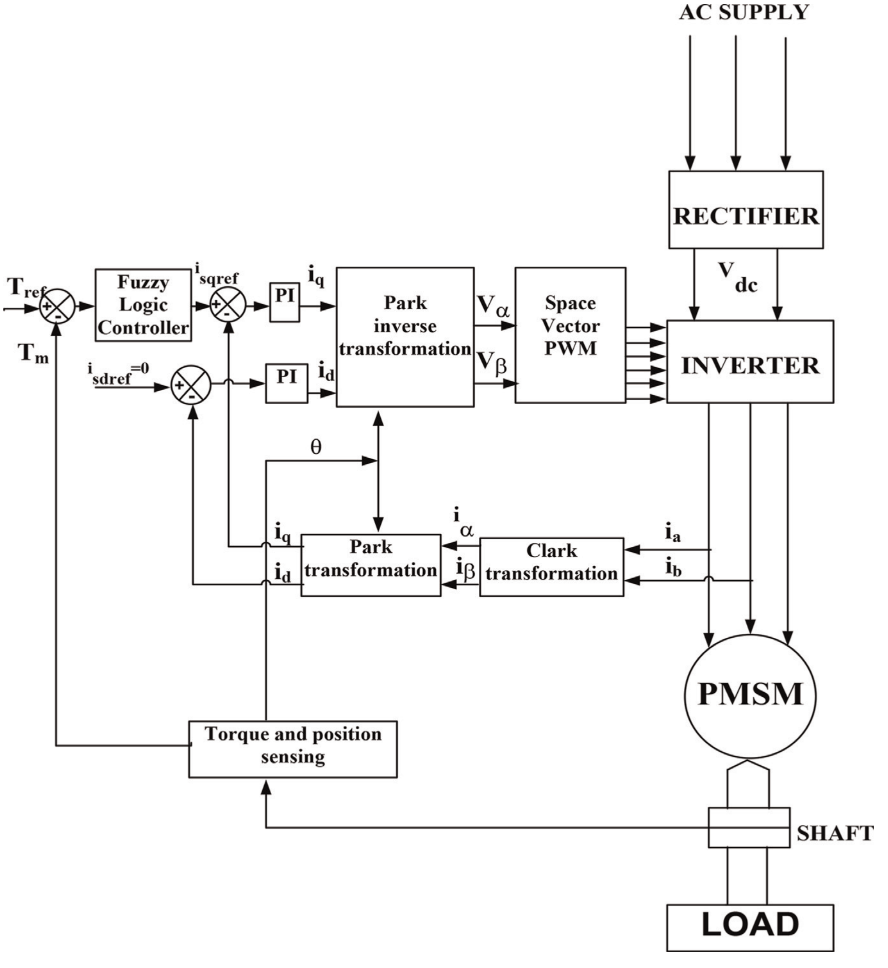

Figure 11.
Block diagram of PMSM driven by FOC using FLC with SVPWM.

5.2.3.1 Space vector pulse width modulation

Space vector PWM (SVPWM) refers to a special technique of determining the switching sequence of the upper three power transistors of a three-phase voltage source inverter (VSI). There are eight possible combinations of on and off states for the three upper power transistors which determine eight phase voltage configurations. This PWM technique controls the motor based on the switching of space voltage vectors, by which an approximate circular rotary magnetic field is obtained. It approximates the reference voltage Vref by a combination of the eight switching patterns (V_0–V_7). The vectors (V_1–V_6) divide the plane into six sectors (each sector: 60°). Vref is generated by two adjacent non-zero vectors and two zero vectors. The switching sector is shown in **Figure 12** and **Table 1** shows the switching vector for inverter.

5.2.3.2 PI controller tuning

The current loop PI controllers compare the actual current with reference current and produce iq and id current, respectively. PI tuning is done by trial and error method.

5.2.3.3 Fuzzy logic controller

The basic concept behind FLC is to utilize the expert knowledge and experience of a human operator for designing a controller an application process whose input-output relationship is given by a collection of fuzzy control rules using linguistic variables instead of a complicated dynamic model.

The FLC initially converts the crisp error and change in error variables into fuzzy variables and then are mapped into linguistic labels. Membership functions are associated with each label as shown in which consists of two inputs and one output. The inputs are Torque error and change in torque error and the output is torque limit. Fuzzy Inference System uses "IF… THEN…" statements, and the

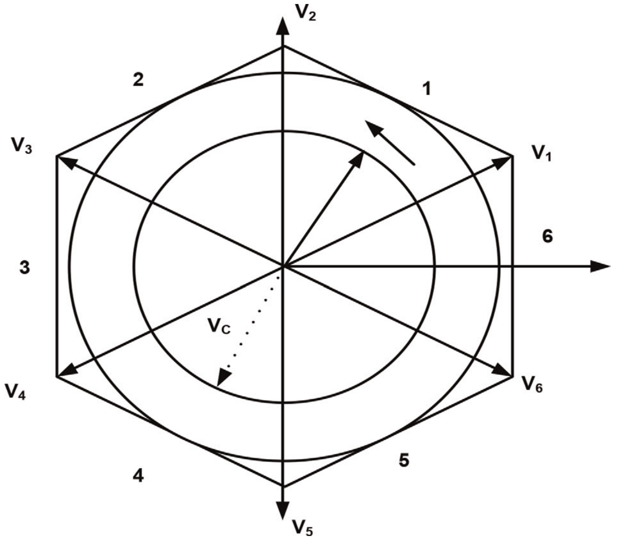

Figure 12.
Switching vectors and sectors.

Vector	A+	B+	C+	A-	B-	C-	VAB	VBC	VCA
V0 = {000}	OFF	OFF	OFF	ON	ON	ON	0	0	0
V1 = {100}	ON	OFF	OFF	OFF	ON	ON	+Vdc	0	−Vdc
V2 = {110}	ON	ON	OFF	OFF	OFF	ON	0	+Vdc	−Vdc
V3 = {010}	OFF	ON	OFF	ON	OFF	ON	−Vdc	+Vdc	0
V4 = {011}	OFF	ON	ON	ON	OFF	OFF	−Vdc	0	+Vdc
V5 = {001}	OFF	OFF	ON	ON	ON	OFF	0	−Vdc	+Vdc
V6 = {101}	ON	OFF	ON	OFF	ON	OFF	+Vdc	−Vdc	0
V7 = {111}	ON	ON	ON	OFF	OFF	OFF	0	0	0

Table 1.
Switching vectors for inverter.

connectors present in the rule statement are “OR” or “AND” to make the necessary decision rules.

The linguistic labels are divided into seven groups. They are: NB—negative big; NM—negative medium; NS—negative small; Z—zero; PS—positive small; PM—positive medium; PB—positive big. Each of the inputs and the output contain membership functions with all these seven linguistics.

Figure 13 shows the speed error, **Figure 14** shows the change in speed error and **Figure 15** shows the torque limit.

The mapping of the fuzzy inputs into the required output is derived with the help of a rule base as given in **Table 2**.

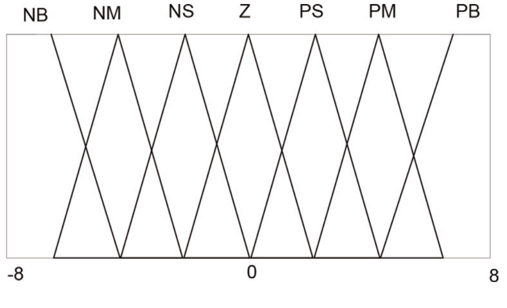

Figure 13.
Torque error input to FLC.

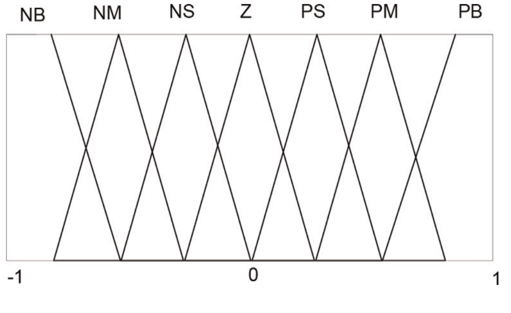

Figure 14.
Change in torque error input to FLC.

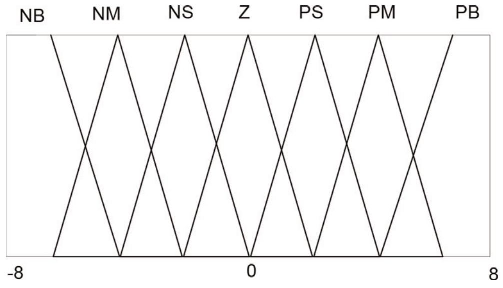

Figure 15.
Torque limit output of FLC.

e Δe	NB	NM	NS	Z	PS	PM	PB
NB	NB	NB	NB	NM	NM	NS	Z
NM	NB	NB	NB	NM	NS	Z	PS
NS	NB	NM	NS	NS	Z	PS	PM
Z	NM	NM	NS	Z	PS	PM	PM
PS	NM	NS	Z	PS	PS	PM	PB
PM	NS	Z	PS	PM	PM	PB	PB
PB	Z	PS	PM	PM	PB	PB	PB

Table 2.
Rules for FLC.

5.2.3.4 Simulation results and discussion

The simulink model of FLC with SVPWM based FOC of PMSM is shown in **Figure 16** and that of SVPWM pulse production is shown in **Figure 17**.

The FOC of PMSM is done using conventional PI controller and FLC using SVPWM techniques using MATLAB version R2009a and the results are compared with other reported results in **Table 3**. The parameters of PMSM used in the simulation are given in the appendix.

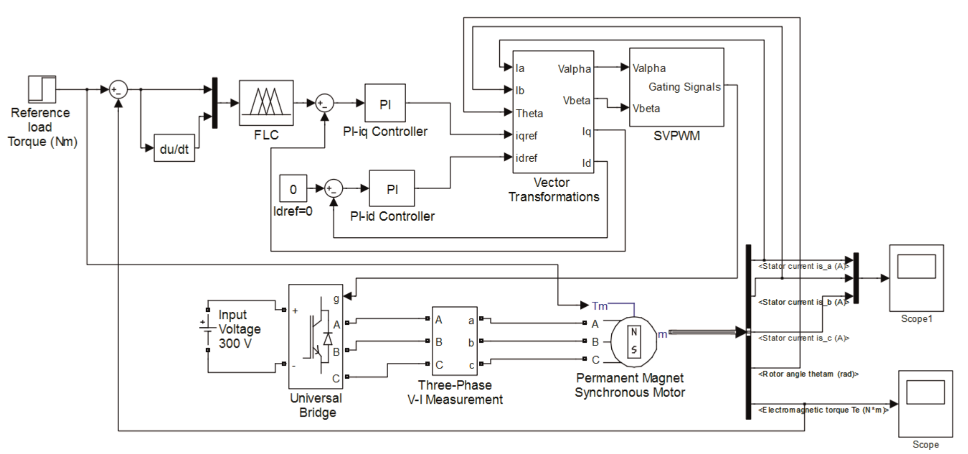

Figure 16.
Simulink model of FLC with SVPWM based FOC of PMSM.

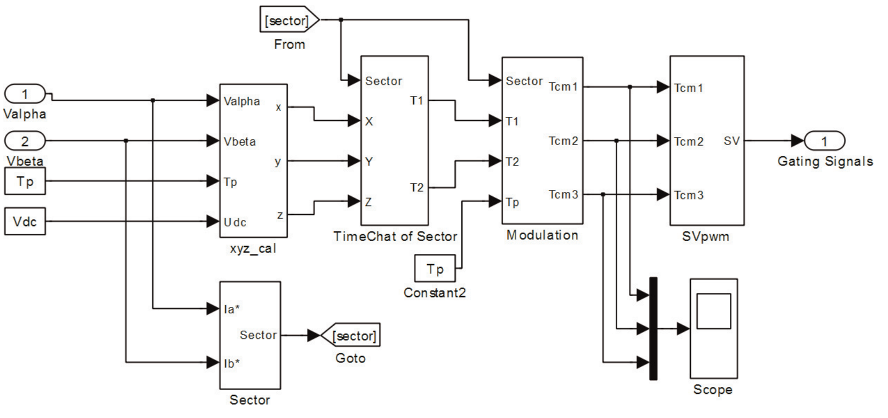

Figure 17.
Simulink model of SVPWM pulse production.

Control strategies	Torque ripple factor (%)
Proposed FLC with SVPWM	1.75
Mattavelli et al. [8]	3.8
Qian et al. [9]	3.9
Tarnik and Murgas [10]	4
Hasanien [11]	12

Table 3.
Comparison of control strategies in PMSM.

The torque ripple can be calculated by using the relation.

$$\text{Torque ripple factor} = \frac{\text{Peak to peak torque}}{\text{Rated torque}} \tag{23}$$

The simulation results are shown in **Figures 18–20**.

From **Figure 19** (Torque waveform) it is inferred that the torque ripples oscillates from 7.91 Nm (minimum) to 8.05 Nm (maximum) for the given reference torque of 8 Nm.

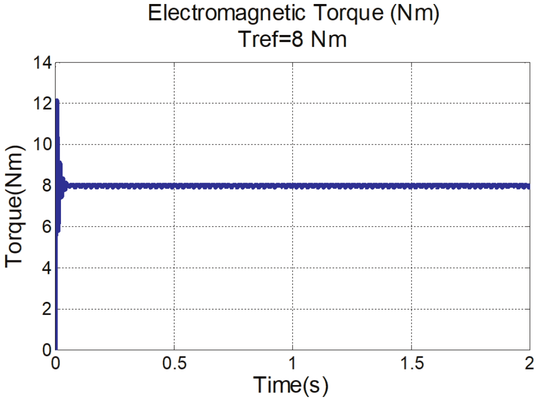

Figure 18.
Torque output for FOC based PMSM using FLC and SVPWM.

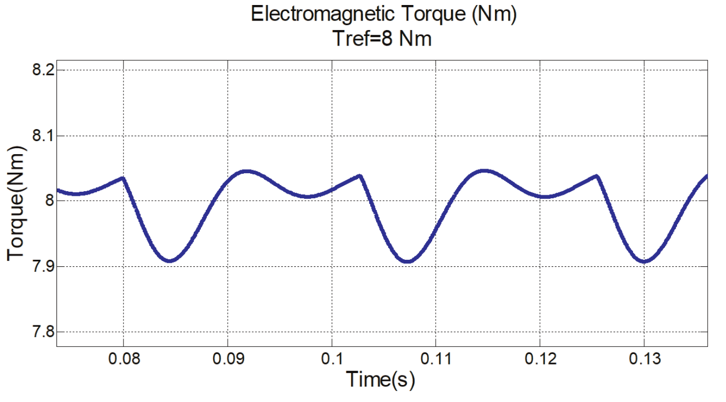

Figure 19.
Torque ripples in FOC based PMSM using FLC and SVPWM.

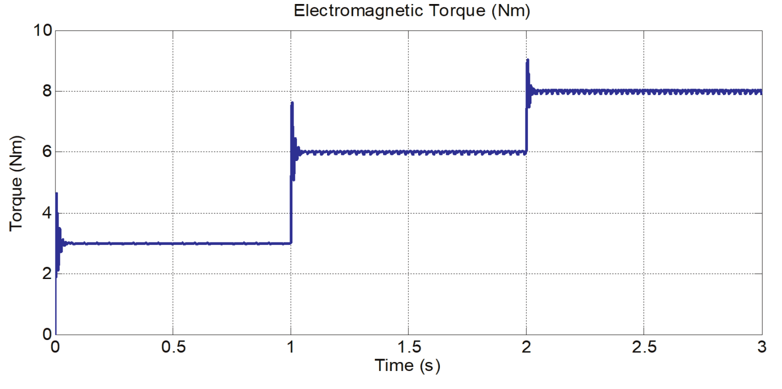

Figure 20.
Dynamic torque using FLC with SVPWM based field controlled PMSM.

Torque ripple factor (%) as per Eq. 23 is given by = ((8.05–7.91)/8) × 100 = 0.14/8 × 100 = **1.75.**

It is clear that variation in torque shown in **Table 3** is less in case of fuzzy logic controllers and they can achieve a minimum torque ripple than other control techniques. It has been viewed that the discussed control strategy has helped in reducing the torque ripples to 1.75%. Thus by using FLC based controller, ripples are reduced completely.

6. Advanced topics in PMSM drives

6.1 PMSM control with rotor position sensors

The encoders, resolvers, eddy current sensors are used for rotor position sensing of PMSM control. Absolute encoder has the advantages that it could retain the position information in power outage conditions and for long inactive periods of devices. It is suitable for the applications such as flow control, crane movement, and astronomical telescopes. The position resolvers are the rotary transformers where primary winding is placed on rotor. The induced voltage at secondary winding is shifted by 90 would be different which is based on the rotor shaft angle [12].

The PMSM control with speed, torque controller, where rotor angular position sensor is used to get the feedback. The general block diagram is given in **Figure 21**.

The PMSM control with speed, torque controller, where rotor angular position sensor is used to get the feedback. The general block diagram is given in **Figure 22**.

6.2 PMSM control without position sensors

The control scheme for sensorless PMSM where the rotor position information is used as feedback to controllers is given in **Figure 23**.

The estimation of stator flux is used to find the stator current at a predicted rotor position. The error in the predicted rotor position is corrected by finding the difference between the estimated stator current and measured current [13].

6.2.1 Sensorless control schemes for PMSM

The difficulties in estimating the rotor position due the reasons: 1. scalar speed estimation and 2. initial position of rotor is not known. The non-measurable variables of PMSM are estimated by the observers. For zero-speed application, salience tracking technique is considered as appropriate, where back-Emf technique fails at low speed. The methods generally used to estimate the rotor position are tracking observer, tracking state filter and arctangent calculation [14].

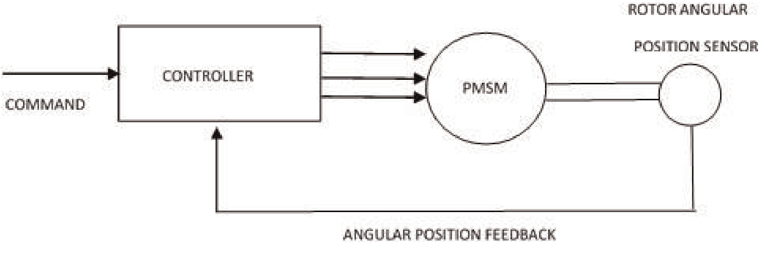

Figure 21.
The general block diagram for PMSM control with rotor position sensor.

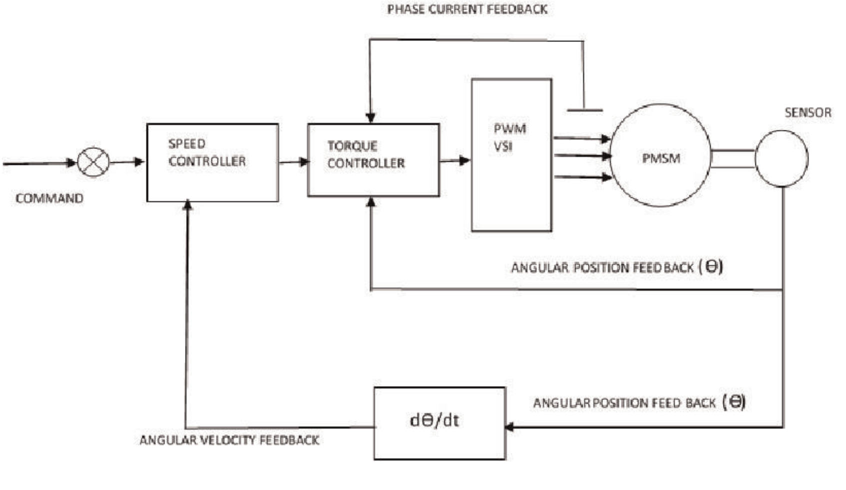

Figure 22.
PMSM control scheme with angular position sensor [13].

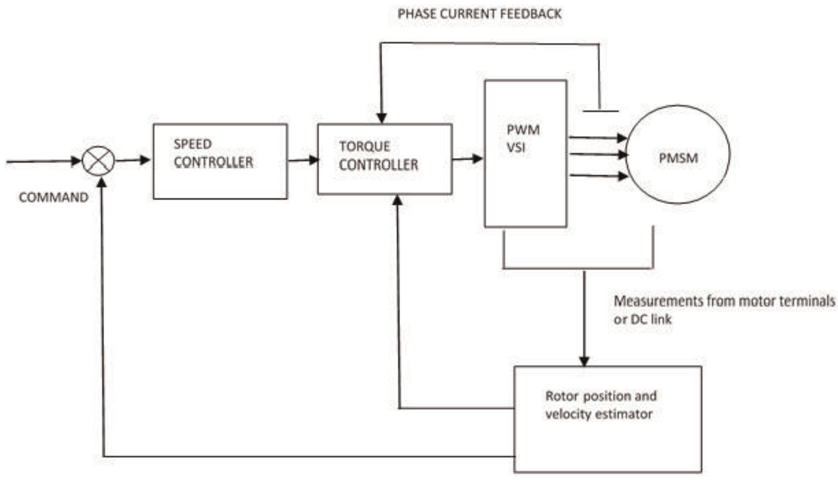

Figure 23.
Sensorless control scheme for PMSM.

The sliding mode observer having sigmoid switching function, effectively suppressed the oscillation of system. The cut-off frequency of LPF is tuned to rotor speed, so that the rotor speed becomes real-time and tunable [15].

In PMSM vector control system with space vector PWM voltage source inverter (SVPVM-VSI), the single shunt current sensing with model reference adaptive system (MRAS) for rotor position sensorless control method is implemented [16].

To estimate the position variable of PMSM: 1. Linear Luenberger observer is constructed 2. PI-type controller which is based on LMI is suggested [17].

To estimate the rotor position: 1. The delta-sigma modulation 2. CIC extraction filter method are used. It is found that signal-to-noise ratio is high in this technique [18].

The neural network observer used for estimating speed/position of rotor in PMSM, where the observer can do the tracking of the rotor speed at low speed range with greater accuracy [19].

A linearized IPMSM model which is using FOC is created. The rotor speed and phase current of the model is estimated by extended Kalman filter (EKF) [20].

A novel SMO is proposed to achieve greater degree of accuracy in estimating the position and speed of PMSM. Further, the observer reduced the filter links and phase compensation links that achieved a simplification in traditional SMO [21].

A simplified vector control model of PMSM with NNPID controller is created. Automatic tuning of variables could be achieved by using BP NNPID. The overswing phenomenon is eliminated to the maximum extent possible [22].

The feasibility of feedback linearization of PMSM model is shown by MIMO nonlinear system example and then it was combined with vector control method. For handling the nonlinear system, it is showed that feedback linearization is a better method and has better control capability [23].

To estimate the initial position of rotor, a start-up strategy is proposed to overcome the drawback of back emf based control at zero and low speed ranges. The NN based controller is employed to control the current and speed of back emf based FOC of PMSM. The dynamic response of surface mounted type PMSM is improved [24].

A model of IPMSM is developed based on intelligent control method maximum torque per ampere (MTPA) principle in order to achieve the dynamic response characteristics for high precision position servo systems. The shakeless fuzzy controller is proposed with a new control method which is based on single neuron that tunes the output scaling factor of the controller [25].

To estimate the rotor position, speed and stator resistance, an interconnected higher order sliding mode observer (HOSMO) for IPMSM is developed [26].

The traditional backstepping control is improved by adding integral control at each step of the tracking and regulation strategies. This permits to reject uncertainties and disturbances.

The stator resistance is influenced by temperature variation that varies randomly. An improved method based on variable parameter PI to compensate the stator resistance is proposed. By constructing the stator flux observer mathematical model of direct torque control (DTC), the problem of error existing in stator flux is solved [27].

6.2.2 Speed-torque ripple-suppression

An ILC controller is implemented along with a PI speed controller to minimize the periodic ripples in speed. When the learning algorithm is implemented in frequency domain, it showed better performance in minimizing the ripples in speed than time domain implementation. This is due to the elimination of forgetting factor (FF), in time domain learning method [28].

A new novel method "Intelligent sensor bearing" is implemented by modifying the feedback information that comes from sensor. An Iterative Learning Control (ILC) is used to deal with the periodical errors for reducing ripples in speed [29].

A novel technique "Instantaneous torque control" based on fuzzy logic controller (FLC) with SVPWM is proposed to reduce the torque ripples in PMSM. The simulation results are presented in Section 5.2.3 [30].

To minimize the torque ripples of PMSM, the instantaneous field oriented torque control schemes (a) ILC with hysteresis pulse width modulation (HPWM), (b) ILC with SVPWM are proposed. The simulation results showed that ILC with SVPWM has better control over torque ripples [31].

The speed torque ripple minimization of PMSM is achieved by using neural networks (NN). The conventional PI-controller based vector control method was compared with feed forward NN (FFNN). The simulation showed that NN controller has better control than PI controller [32].

6.2.3 Application specific PMSM controls

In high speed traction applications, the motor speed range of IPMSM is extended by single current regulator flux-weakening control strategy which results in steady operation of motor with high speed [29].

Acknowledgements

We thankful to the management and School of Electrical and Mechanical Engineering of Addiss Ababa Science and Technology University, Addiss Ababa, Ethiopia for their encouragement, support and facilities provided for our book chapter work.

Nomenclature

f_c	crossover frequency
i_d	d-axis current
L_{dm}	d-axis magnetizing inductance

DOI: http://dx.doi.org/10.5772/intechopen.88597

L_d	d-axis self-inductance
V_d	d-axis voltage
ρ	derivative operator
T_e	develop electromagnetic torque
d	direct or polar axis
DTC	direct torque control
ω_r	electrical speed
i_f	equivalent permanent magnet field current
L_s	equivalent self-inductance per phase
λ_d	flux linkage due d axis
λ_q	flux linkage due q axis
λ_{dm}	flux linkage due to rotor magnets linking the stator
B	friction
FLC	fuzzy logic controller
J	inertia
k_i	integral control gain
T_L	load torque
ω_{rated}	motor rated speed
T_m	motor torque
P	number of poles
I_m	peak value of supply current
λ_f	PM flux linkage or field flux linkage
k_p	proportional control gain
i_q	q-axis current
L_{qm}	q-axis magnetizing inductance
L_q	q-axis self-inductance
V_q	q-axis voltage
q	quadrature or interpolar axis
T_{ref}	reference motor torque
θ_r	rotor position
ω_m	rotor speed
L	self-inductance
L_{ls}	stator leakage inductance
R_s	stator resistance
i_a, i_b, i_c	three phase currents
V_a, V_b, V_c	three phase voltage

Appendix 1: parameters of PMSM

Rated power	1 HP
Rated torque	8 Nm
Rated voltage	300 V
Rated current	2.5 A
Stator resistance	0.9585 Ω
Inductance L_d	0.00525 H
Inductance L_q	0.00525 H
Magnetic flux	0.1827 weber
No. of poles	8

Moment of inertia	0.0006329 kg m^2
Friction factor	0.0003035 Nm/(rad/s)

Appendix 2: block parameters

kp	10
ki	1

Author details

Adhavan Balashanmugham[1*] and Mockaisamy Maheswaran[2]

1 Department of Electrical and Computer Engineering, Addis Ababa Science and Technology University, Addis Ababa, Ethiopia

2 Department of Electromechanical Engineering, Addis Ababa Science and Technology University, Addis Ababa, Ethiopia

*Address all correspondence to: adhav14@gmail.com

References

[1] Bimbra PS. Electric Machinery. 7th ed. Delhi, India: Khanna Publishers; 2011. p. 1060. ISBN: 978-8174091734

[2] Bose BK. Power Electronics and Variable Frequency Drives. 1st ed. NJ, USA: Wiley John & Sons; 1996. p. 660. ISBN: 978-0-780-31084-1

[3] Krishnan R. Electric Motor Drives Modeling, Analysis, and Control. NJ, USA: Prentice Hall; 2011. p. 652. ISBN: 9780130910147

[4] Bose BK. Modern Power Electronics and AC Drives. NJ, USA: Prentice Hall; 2002. p. 738. ISBN: 9780130167436

[5] Pillay P, Krishnan R. Modeling of permanent magnet motor drives. IEEE Transactions on Industrial Electronics. 1988;**354**:537-541. DOI: 0278-0046/88/1100-0537

[6] The MathWorks Incorporation. SimPowerSystems™ User's Guide [Internet]. 2013. Available from: http://www.mathworks.in/help/pdf_doc/physmod/powersys/powersys.pdf [Accessed: 10 June 2019]

[7] Novotny DW, Lipo TA. Vector Control and Dynamics of AC Drives. New York, USA: Oxford University Press; 1998. p. 456. ISBN: 9780198564393

[8] Mattavelli P, Tubiana L, Zigliotto M. Torque-ripple reduction in PM synchronous motor drives using repetitive current control. IEEE Transactions on Power Electronics. 2005:1423-1431

[9] Qian W, Panda SK, Xu JX. Torque ripple minimization in PM synchronous motors using iterative learning control. IEEE Transactions on Power Electronics. 2004:272-279

[10] Tarnik M, Murgas J. Additional adaptive controller for mutual torque ripple minimization in PMSM drive systems. In: Ni Y-Q, Ye X-W, editors. Proceedings of 18th IFAC World Congress. Milano, Italy; 2011. pp. 4119-4124

[11] Hasanien H. Torque ripple minimization of permanent magnet synchronous motor using digital observer controller. Energy Conversion and Management. 2010:98-104

[12] Kiran N, Anitha Nair AS, Sri Lakshmi D. Permanent magnet synchronous motor control with speed feedback using a resolver. International Journal of Advanced Research in Education and Technology (IJARET). 2016;**3**(4):74-78

[13] Chandana Perera PD. Sensorless control of permanent-magnet synchronous motor drives [thesis]. Denmark: Aalborg University; 2002

[14] Glumineau A, de León Morales J. Sensorless AC Electric Motor Control Robust Advanced Design Techniques and Applications. Switzerland: Springer International Publishing; 2015. pp. 121-137. DOI: 10.1007/978-3-319-14586-0-4

[15] Hu W, editor. Electronics and Signal Processing. Berlin, Heidelberg: Springer-Verlag; 2011. pp. 533-538. DOI: 10.1007/978-3-642-21697-8

[16] Ma H, Wang W, editors. Mechatronics and Automatic Control Systems. Heidelberg, New York, Dordrecht, London: Springer Cham; 2014. pp. 727-732. DOI: 10.1007/978-3-319-01273-5

[17] Sun X, Yi Y, Cao S, Liu H, Zhang T. Robust PI-type position controller design for permanent magnet synchronous motor using LMI techniques. In: Deng Z, Li H, editors.

Proceedings of the 2015 Chinese Intelligent Automation Conference. Berlin, Heidelberg: Springer-Verlag; 2015. pp. 405-410. DOI: 10.1007/978-3-662-46463-2

[18] Zhu B, Zhao H, Zhu J, He Y. Design and implementation of a PMSM rotor position detecting system with high speed and high precision. In: Deng Z, Li H, editors. Proceedings of the 2015 Chinese Intelligent Automation Conference. Berlin, Heidelberg: Springer-Verlag; 2015. pp. 513-518. DOI: 10.1007/978-3-662-46463-2

[19] Shoeb Hussain, Mohammad Abid Bazaz. Sensorless control of PMSM drive with neural network observer using a modified SVPWM strategy. In: Juan Manuel Corchado Rodriguez, Sushmita Mitra, Sabu M. Thampi, El-Sayed El-Alfy, editors. Intelligent Systems Technologies and Applications. Springer International Publishing AG; 2016. p. 857–862. DOI 10.1007/978-3-319-47952-1.

[20] Mathianantham L, Gomathi V, Ramkumar K, Balasubramanian G. State estimation of interior permanent magnet synchronous motor drives using EKF. In: Suresh LP, Panigrahi BK, editors. Proceedings of the International Conference on Soft Computing Systems. India: Springer; 2016. pp. 719-724. DOI: 10.1007/978-81-322-2671-0

[21] Zhu X. Research on sensorless control of PMSM based on a novel sliding mode observer. In: Deng Z, editor. Proceedings of 2017 Chinese Intelligent Automation Conference. Singapore Pte Ltd.: Springer Nature; 2108. pp. 193-198. DOI: 10.1007/978-981-10-6445-6

[22] Zhang L, Xu B-J, Wen K-L, Li Y-H. The study of permanent magnetic synchronous motor control system through the combination of BP neural network and PID control. In: Juang J, Huang Y-C, editors. Intelligent Technologies and Engineering Systems. Heidelberg, New York, Dordrecht, London: Springer; 2013. pp. 311-316. DOI: 10.1007/978-1-4614-6747-2

[23] Wang H, Liu X. Permanent magnet synchronous motor, feedback linearization vector control. In: Ma H, Wang W, editors. Mechatronics and Automatic Control Systems. Cham, Heidelberg, New York, Dordrecht, London: Springer; 2014. pp. 601-606. DOI: 10.1007/978-3-319-01273-5

[24] Nagarajan VS, Subashini TS. Back-emf-based sensorless field oriented control of PMSM using neural-network-based controller with a start-up strategy. In: Suresh LP, Dash SS, Panigrahi BK, editors. Artificial Intelligence and Evolutionary Algorithms in Engineering Systems. India: Springer; 2015. pp. 449-454. DOI: 10.1007/978-81-322-2135-7

[25] Shao M, Yu H, Wang Z, Xie H, Zhao S. Position control of interior permanent synchronous motor based on improved shakeless fuzzy controller. In: Deng Z, Li H, editors. Proceedings of the 2015 Chinese Intelligent Automation Conference. Berlin, Heidelberg: Springer-Verlag; 2015. pp. 83-88. DOI: 10.1007/978-3-662-46463-2

[26] Glumineau A, de Leon Morales J. Sensorless AC Electric Motor Control Robust Advanced Design Techniques and Applications. Switzerland: Springer International Publishing; 2015. pp. 112-117. DOI: 10.1007/978-3-319-14586-0-4

[27] Zhang S, Cui W, Shen Y, Liu H. Direct torque control of permanent magnet synchronous motor at low speed using a variable PI feedback flux observer. In: Huang B, Yao Y, editors. Proceedings of the 5th International Conference on Electrical Engineering and Automatic Control. Berlin, Heidelberg: Springer-Verlag; 2016.

pp. 927-932. DOI: 10.1007/978-3-662-48768-6

[28] Xu J-X, Panda SK, Lee TH, editors. Real-Time Iterative Learning Control Design and Applications. London: Springer-Verlag; 2009. pp. 101-106. DOI: 10.1007/978-1-84882-175-0.

[29] Hu T, Lin F, Cui L, Yuan Q, Yang Z. The flux-weakening control of interior permanent magnet synchronous traction motors for high-speed train. In: Ni Y-Q, Ye X-W, editors. Proceedings of the 1st International Workshop on High-Speed and Intercity Railways. Berlin, Heidelberg: Springer-Verlag; 2012. pp. 451-461. DOI: 10.1007/978-3-642-27960-7

[30] Adhavan B, Birundha MS, Ravichandran CS, Jagannathan V. Torque ripple reduction in PMSM using FLC. Australian Journal of Basic and Applied Sciences. 2013;**61**(2):61-68. ISSN 1991-8178

[31] Adhavan B, Jagannathan V. Performance comparison of hysteresis pulse width modulation and space vector pulse width modulation technique for torque ripple reduction in permanent magnet synchronous motor using iterative learning control. Journal of Vibration and Control. 2012;**20**(5): 698-712. DOI: 10.1177/1077546312463748

[32] Adhavan B, Jagannathan V. Torque ripple minimization in permanent synchronous motor using neural networks. Advances in Modelling and Analysis C Automatic Control. 2013;**68** (2):65-80. ISSN: 1240-4535